

Cell Reports, Volume 23

Supplemental Information

**Role of Selenof as a Gatekeeper
of Secreted Disulfide-Rich Glycoproteins**

Sun Hee Yim, Robert A. Everley, Frank A. Schildberg, Sang-Goo Lee, Andrea Orsi, Zachary R. Barbati, Kutay Karatepe, Dmitry E. Fomenko, Petra A. Tsuji, Hongbo R. Luo, Steven P. Gygi, Roberto Sitia, Arlene H. Sharpe, Dolph L. Hatfield, and Vadim N. Gladyshev

SUPPLEMENTAL INFORMATION

Supplemental Figures

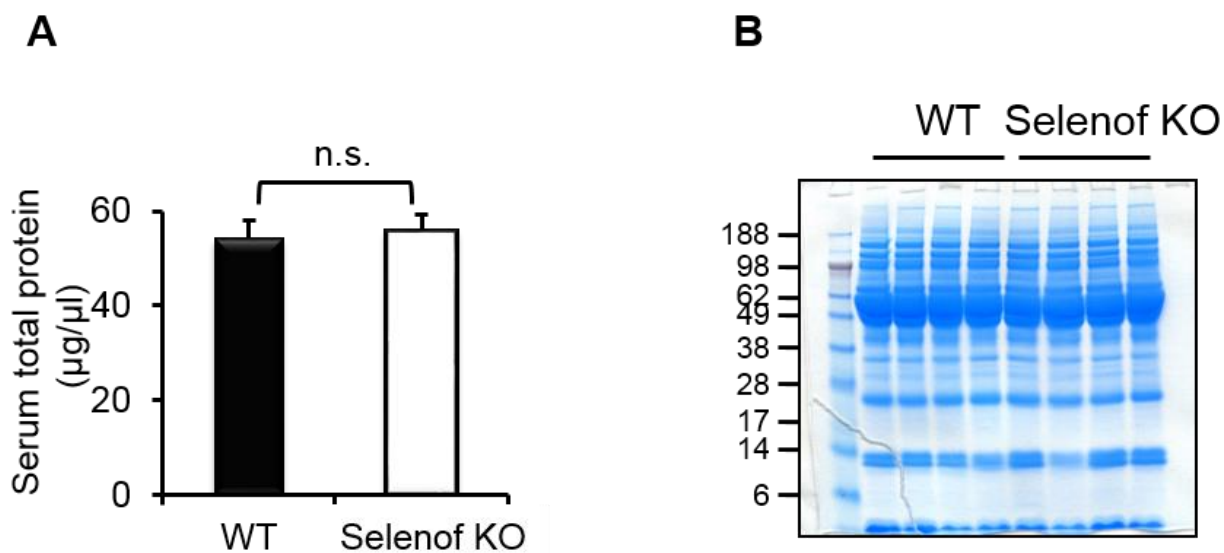


Figure S1. Selenof deficiency does not affect protein levels in plasma, related to Fig. 1. (A) Total protein in the sera of WT and Selenof KO mice. The serum protein concentration of WT mice was 54.2 ± 3.81 $\mu\text{g}/\mu\text{l}$ and Selenof KO was 55.81 ± 3.39 $\mu\text{g}/\mu\text{l}$ ($p=0.32$, $n=10$ per group). (B) Protein staining of the sera from WT and Selenof KO mice analyzed by SDS-PAGE.

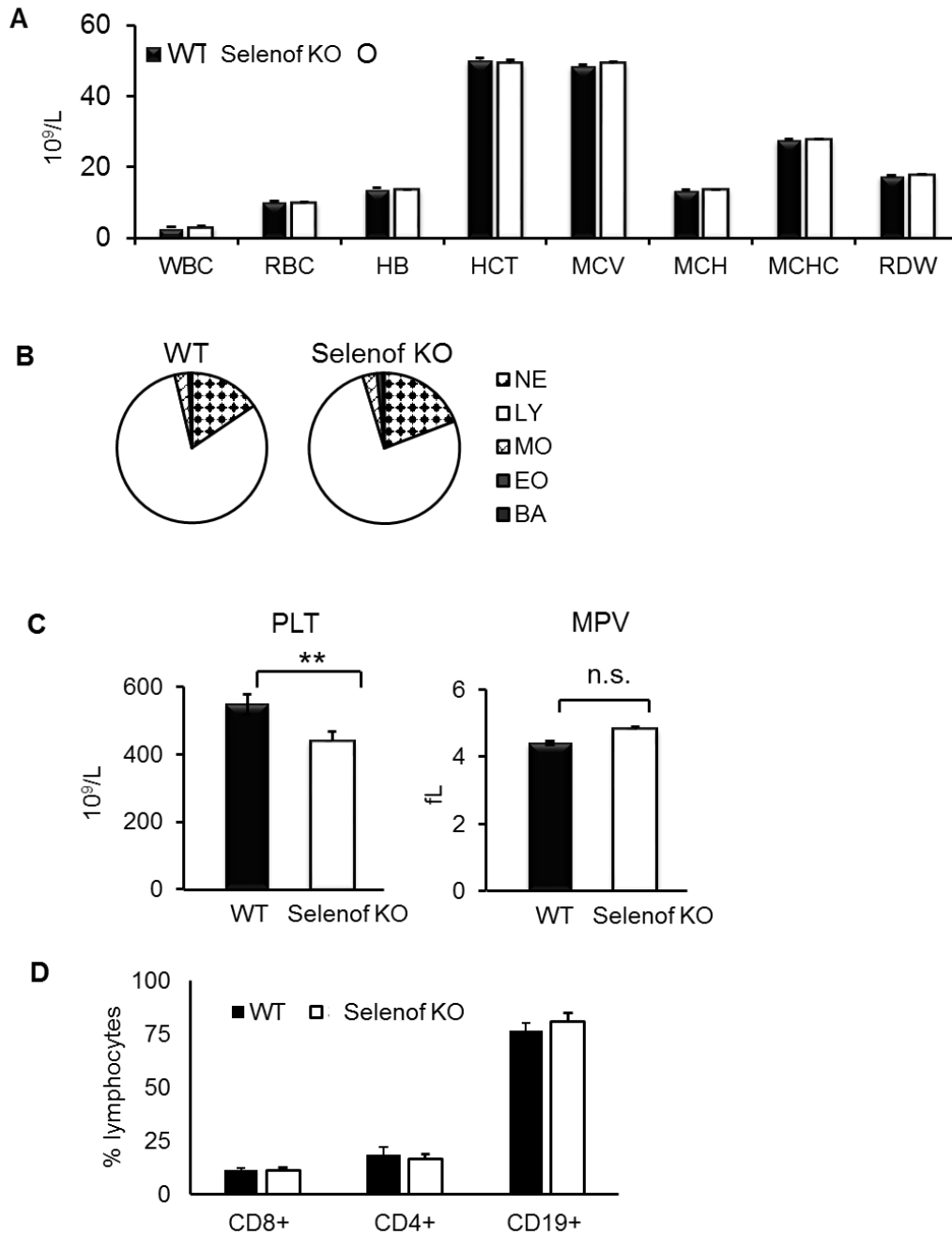


Figure S2. Selenof deficiency leads to a decrease in platelet count, related to Fig. 1. (A) Complete blood analyses using Hemavet Systems are shown for WT and Selenof KO mice (n=10 per group, 12-week-old male mice), including (B) neutrophils (polys and bands) (NE); lymphocytes (LY); monocytes (MO); eosinophils (EO); and basophils (BA). Units of measurement: (A) WBC (total white blood cells, K/ μ L), RBC (total red blood cells, M/ μ L), HB (hemoglobin, g/dL), HCT (Hematocrit, %), MCV (mean corpuscular volume, fL), MCH (mean corpuscular hemoglobin, pg), MCHC (mean corpuscular hemoglobin concentration, g/dL), RDW (RBC distribution width, %), (C) PLT (platelet count, K/ μ L), MPV (mean platelet volume, fL). (D) Percent of CD8+, CD4+, and CD19+ cells (% in lymphocytes).

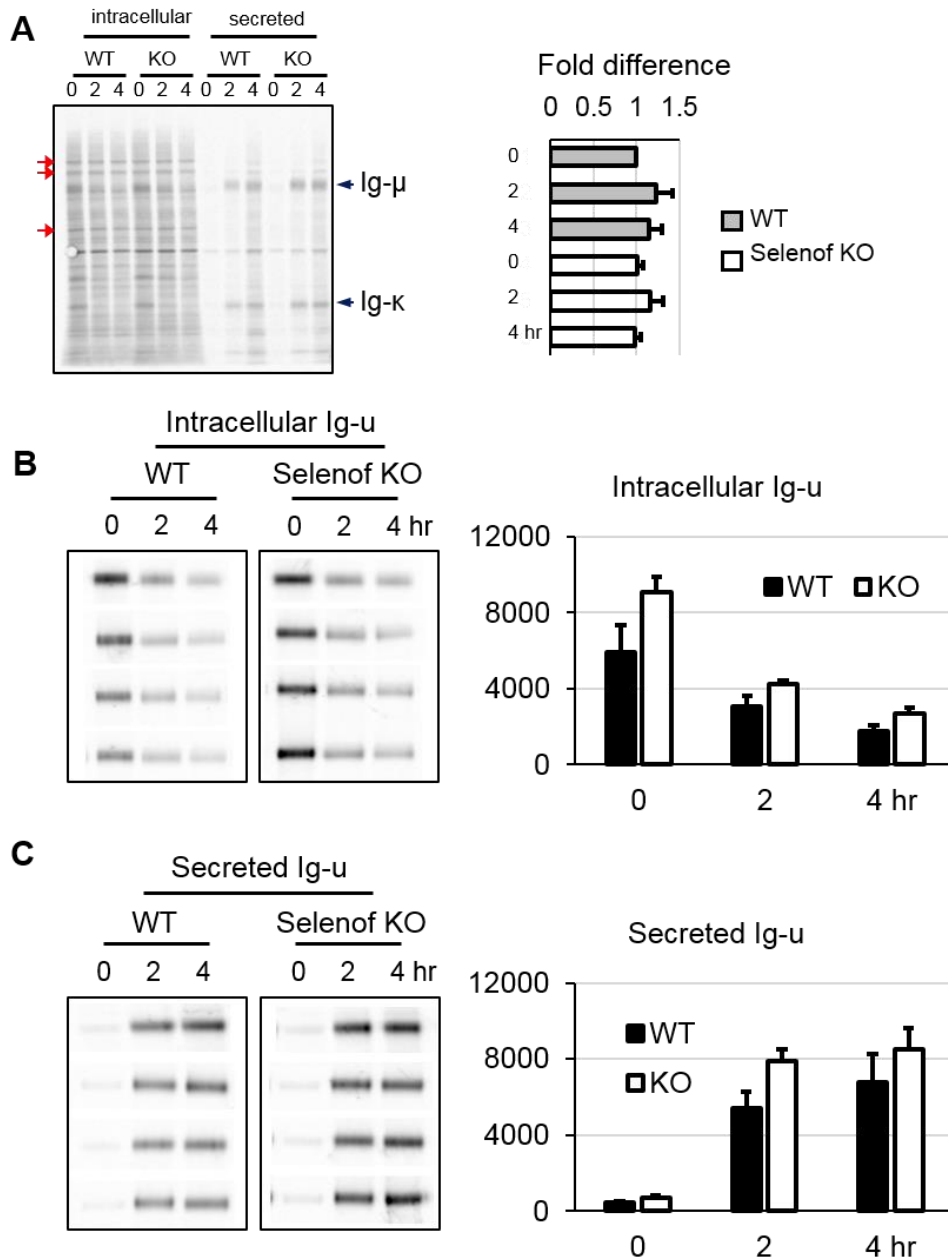


Figure S3. Kinetics of IgM biosynthesis and transport by radioactive pulse-chase assay, related to Fig. 2. (A) Intracellular and secreted proteins resolved in SDS-PAGE at differentiating day 3 plasma B cells isolated from WT and Selenof KO mice. Same number of cells were used for the analyses and additional protein quantification was accessed with levels of non-specific bands (marked with red arrows). (B) Intracellular Ig- μ and (C) secreted Ig- μ were measured under reducing conditions from biological and technical replicate samples. The Ig- μ expression levels were measured and compared using ImageJ. The artificial units were used in x-axis.

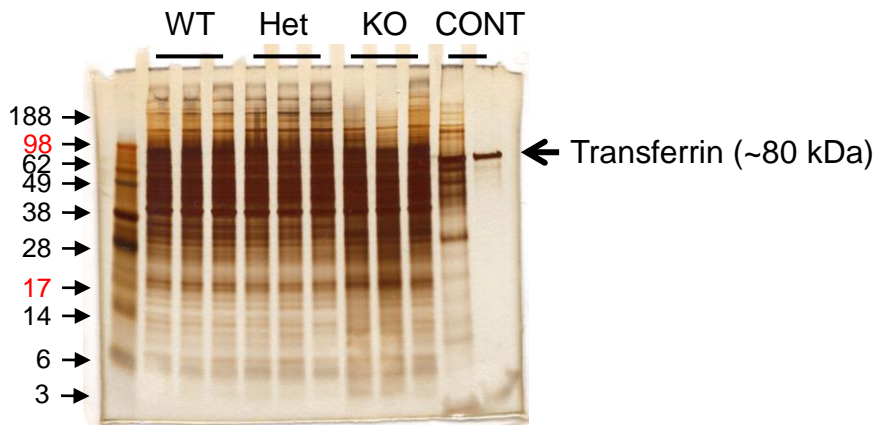


Figure S4. Silver stained proteins from cell pellets of Selenof MEFs, related to Fig. 6. WT, heterozygous (Het), and Selenof KO MEFs were cultured under serum starvation conditions. Lane 1; protein markers, lanes 2-4; WT MEFs, lanes 5-7; Het MEFs, lanes 8-10; KO MEFs, lane 11; concentrated cell culture medium obtained from WT MEFs, and lane 12; concentrated fresh culture medium (equal volume with lane 11) which was supplemented with insulin, transferrin, and selenium.

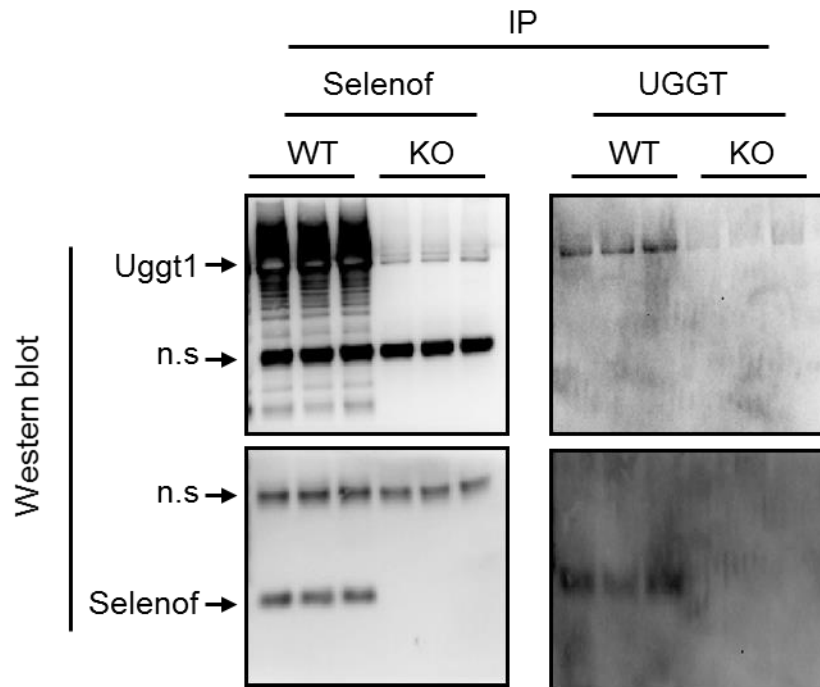


Figure S5. Selenof interaction with UGGT1, related to Fig. 6. Cell lysates from livers of WT and KO mice (3 animals per group) were subjected for immunoprecipitation with anti-Selenof or anti-UGGT1 antibodies. The IP products were characterized by Western blot analysis using anti-Selenof or anti-UGGT1 antibodies. Bands at ~15 kDa (Selenof) and ~170 kDa (UGGT1) were observed (indicated by arrows). Non-specific bands (n.s.) correspond to the antibody light chain (~25 kDa) and heavy chain (~ 50 kDa).

Supplemental Tables

Table S1, related to Table 1. Pathway enrichment analysis of proteins downregulated in Selenof KO MEFs.

Pathway name	Proteins found	Proteins Total	Ratio	p-value	FDR
Antigen Presentation: Folding, assembly and peptide loading of class I MHC	11	118	0.011	9.89E-07	0.000591
Antigen processing-Cross presentation	12	176	0.016	7.65E-06	0.0018
Endosomal/Vacuolar pathway	9	97	0.009	1.02E-05	0.0018
ER-Phagosome pathway	11	154	0.014	1.21E-05	0.0018
Interferon alpha/beta signaling	8	138	0.013	7.55E-04	0.0789
Interferon gamma signaling	9	174	0.016	7.96E-04	0.0789
Class I MHC mediated antigen processing & presentation	13	368	0.033	2.00E-03	0.169
WNT5A-dependent internalization of FZD2, FZD5 and ROR2	2	5	0	2.29E-03	0.169
PCP/CE pathway	6	98	0.009	2.64E-03	0.174
Signaling by NOTCH1 t(7;9)(NOTCH1:M1580_K2555) Translocation Mutant	2	8	0.001	5.71E-03	0.308
Constitutive Signaling by NOTCH1 t(7;9)(NOTCH1:M1580_K2555) Translocation Mutant	2	8	0.001	5.71E-03	0.308
Sema4D induced cell migration and growth-cone collapse	3	28	0.003	7.25E-03	0.33
Interferon Signaling	10	289	0.026	7.47E-03	0.33
Beta-catenin independent WNT signaling	7	162	0.015	7.87E-03	0.33
Laminin interactions	3	31	0.003	9.54E-03	0.372
Zinc influx into cells by the SLC39 gene family	2	11	0.001	1.05E-02	0.372
Non-integrin membrane-ECM interactions	4	61	0.006	1.08E-02	0.372
Sema4D in semaphorin signaling	3	33	0.003	1.13E-02	0.372
Semaphorin interactions	4	73	0.007	1.95E-02	0.427
Constitutive Signaling by NOTCH1 HD Domain Mutants	2	16	0.001	2.12E-02	0.427

Table S2, related to Table 1. Pathway enrichment analysis of proteins upregulated in Selenof KO MEFs.

Pathway name	Proteins found	Proteins Total	Ratio	p-value	FDR
COPII (Coat Protein 2) Mediated Vesicle Transport	6	75	0.007	1.29E-04	0.0233
ER to Golgi Anterograde Transport	8	157	0.014	2.18E-04	0.0233
MHC class II antigen presentation	7	141	0.013	6.34E-04	0.0545
Transport to the Golgi and subsequent modification	8	212	0.019	1.52E-03	0.108
Kinesins	4	50	0.005	1.79E-03	0.109
5-Phosphoribose 1-diphosphate biosynthesis	2	9	0.001	3.91E-03	0.19
Laminin interactions	3	31	0.003	4.05E-03	0.19
Cargo concentration in the ER	3	37	0.003	6.58E-03	0.257
Membrane Trafficking	9	340	0.031	8.09E-03	0.275
COPI Mediated Transport	2	14	0.001	9.16E-03	0.275
Golgi to ER Retrograde Transport	2	14	0.001	9.16E-03	0.275
Asparagine N-linked glycosylation	9	377	0.034	1.51E-02	0.38
Fatty Acyl-CoA Biosynthesis	4	95	0.009	1.65E-02	0.38
Recycling pathway of L1	3	53	0.005	1.72E-02	0.38
Regulation of PAK-2p34 activity by PS-GAP/RHG10	1	2	0	2.01E-02	0.38
XBPI(S) activates chaperone genes	4	102	0.009	2.08E-02	0.38
IRE1alpha activates chaperones	4	106	0.01	2.35E-02	0.38
ERK/MAPK targets	2	25	0.002	2.72E-02	0.38
Nuclear Events (kinase and transcription factor activation)	2	28	0.003	3.34E-02	0.427
Association of TriC/CCT with target proteins during biosynthesis	2	30	0.003	3.79E-02	0.427

Table S3, related to Table 1. Enriched functions identified by DAVID. Proteins whose expression differs between WT and Selenof KO MEFs under conditions of serum deprivation were analyzed for functional annotation clustering and the top three clusters are shown in the table.

Annotation Cluster 1	Enrichment Score: 3.65	Count	p-value	Benjamini
GOTERM_BP_FAT	Golgi vesicle transport	10	4.20E-05	6.70E-02
GOTERM_CC_FAT	cytoplasmic membrane-bounded vesicle	20	1.10E-04	1.00E-02
GOTERM_CC_FAT	membrane-bounded vesicle	20	1.70E-04	9.40E-03
GOTERM_CC_FAT	cytoplasmic vesicle	21	2.90E-04	1.00E-02
GOTERM_CC_FAT	vesicle	21	5.00E-04	1.40E-02
GOTERM_BP_FAT	vesicle-mediated transport	18	1.00E-03	4.30E-01
Annotation Cluster 2	Enrichment Score: 2.84	Count	p-value	Benjamini
GOTERM_BP_FAT	Golgi vesicle transport	10	4.20E-05	6.70E-02
GOTERM_CC_FAT	Golgi apparatus	26	1.80E-04	7.10E-03
GOTERM_BP_FAT	intracellular transport	20	6.50E-04	4.10E-01
GOTERM_BP_FAT	vesicle-mediated transport	18	1.00E-03	4.30E-01
SP_PIR_KEYWORDS	protein transport	15	1.10E-03	3.50E-02
GOTERM_BP_FAT	protein transport	21	1.50E-03	4.00E-01
GOTERM_BP_FAT	establishment of protein localization	21	1.70E-03	3.80E-01
GOTERM_BP_FAT	protein localization	22	3.80E-03	5.00E-01
SP_PIR_KEYWORDS	transport	31	5.70E-03	1.20E-01
GOTERM_BP_FAT	cellular protein localization	13	6.00E-03	5.40E-01
GOTERM_BP_FAT	cellular macromolecule localization	13	6.40E-03	5.30E-01
GOTERM_BP_FAT	intracellular protein transport	12	8.00E-03	5.60E-01
Annotation Cluster 3	Enrichment Score: 2.02	Count	p-value	Benjamini
GOTERM_BP_FAT	protein complex assembly	15	4.90E-03	5.20E-01
GOTERM_BP_FAT	protein complex biogenesis	15	4.90E-03	5.20E-01
GOTERM_BP_FAT	protein homooligomerization	6	7.10E-03	5.40E-01
GOTERM_BP_FAT	macromolecular complex subunit organization	18	8.50E-03	5.60E-01
GOTERM_BP_FAT	macromolecular complex assembly	16	2.10E-02	7.70E-01
GOTERM_BP_FAT	protein oligomerization	7	2.30E-02	7.60E-01

Supplemental Experimental Procedures

Western blotting. Total MEF and tissue proteins were prepared using protein lysis buffer containing protease inhibitor cocktails. For immunoblots, lysates were separated on NuPage Novex (10%) or Native PAGE (4-16%) Bis-Tris Gel system, typically 30 µg protein per lane, and transferred onto PVDF membranes. Membranes were incubated with 5% non-fat milk prior to incubation with primary antibodies for 4°C overnight. Blots were visualized using ECL Western Blotting Substrate and BioRad-ChemiDoc XRS+ molecular imager.

Microarray and Ingenuity Pathway Analyses. mRNA was isolated from spleens using Trizol, and microarray analyses were performed on Affymetrix Mouse 430_2.0A gene chips containing 45,000 gene probes. Three individual arrays were analyzed per genotype, and grouped results were compared by ANOVA using mAdb (NCI, NIH, Bethesda, MD). Those genes significantly different from the WT mice ($p < 0.05$) were subjected to Ingenuity Pathway Analysis (Redwood City, CA), which significantly linked genes according to functional biological processes.

Plasma B cell immunoglobulin production assay. Secreted IgM levels during plasma B cell activation were measured daily using ELISA. Each day, a portion of differentiating plasma B cells were washed with PBS and OptiMem Medium by centrifugation. The cell pellets were resuspended in OptiMem medium and counted at a cell density of 1×10^6 cells/ml. Differentiating B cells were then cultured in OptiMem medium to secrete immunoglobulin. After 4 h, the cells and culture media were centrifuged twice at 300 g for 5 min, the spun media were saved and supplemented with protease inhibitors and 10 mM NEM. The secreted IgM levels were accessed from cell-free, centrifuged media using ELISA.

Enzyme-linked immunosorbent assay. Analysis of antigen-specific immunoglobulin titers in serum and B cell culture media was performed with capture ELISA. ELISA plates were prepared by pre-coating with capture antibodies, either rabbit anti-mouse Ig μ -chain or goat anti-mouse Ig (H+L) antibodies. To access the secreted immunoglobulin levels during plasma B cell differentiation, aliquots of diluted (1:10) media obtained from plasma B cell immunoglobulin secretion assay were added to anti-Ig μ -chain coated plates and incubated overnight at 4°C. After extensive washes, anti- μ -HRP (1:1,000) was added and incubated for 1 h at room temperature. The assay was developed with Sigma OPD fast read and the plates were read at 450 nm.

The WT and Selenof KO sera were used to determine immunoglobulin levels. Sera were diluted at 1:12,000 or 1:50,000 to determine immunoglobulin levels using anti-mouse Ig μ -chain coated plates or anti-Ig(H+L) coated plates, respectively. Detecting antibodies were either goat anti-mouse Ig κ -chain HRP or a series of immunoglobulin antibodies, and the plates were read at 450 nm using a plate reader.

Flow cytometry. For the staining of cell surface molecules, splenocytes or cultured cells from *in vitro* experiments were stained in FACS buffer (PBS, 1% FBS, 2 mM EDTA) with saturating concentrations of antibodies against indicated antigens at 4 °C. For intracellular staining, cells were fixed and permeabilized using the Foxp3 fix/perm kit (eBioscience) according to the manufacturer's instructions. Fc gamma receptor blocking antibody (anti-CD16/CD32) was added to prevent non-specific binding and dead cells were excluded from the analysis by using LIVE/DEAD fixable dead cell stain (Thermo Fisher). Flow cytometry was performed on an LSR II instrument (BD Biosciences) and data were analyzed using FlowJo v10.1 (FlowJo, LLC). In some experiments, B cells were purified, *in vitro* stimulated with LPS as described above, and the distribution of surface and intracellular IgM was analyzed at the indicated time points.

Neutrophil isolation for bacteria killing assay. Murine bone-marrow derived neutrophils were isolated from 12-week old C57BL/6J WT male animals. Hind limbs were aseptically harvested, the distal tips of each extremity were severed and bone marrow cells were flushed from femurs and tibias. Neutrophils from mouse bone marrow cells were isolated using negative depletion of other cell populations with a Neutrophil Isolation Kit (Miltenyi Biotec). The purity of neutrophils, as determined by Wright-Giemsa-staining method, was consistently greater than 98%.

***In vitro* bacteria killing assay.** Blood was withdrawn from the submandibular vein of WT and Selenof KO male mice, and the sera were separated using BD Microtainer serum separator tubes. Fresh overnight cultures of *S. aureus* (ATCC strain 10390) and *E. coli* (ATCC strain 19138) grown in Luria-Bertani medium were diluted 10-fold with fresh LB culture media and incubated for an additional 2 h at 37 °C. Bacteria were pelleted by centrifugation, washed twice with PBS, and resuspended in PBS at an OD = 0.2 at 600 nm. Bacteria were opsonized with 10% (v/v) WT or Selenof KO mouse serum for 1 h at 37 °C on an end-to-end rotator. The opsonized bacteria and neutrophils obtained from WT animals were mixed together at a 1:5 ratio for *E. coli* and 1:10 ratio for *S. aureus* (calculated by cell numbers) and incubated for 0, 30, 60 and 120 min at 37 °C with intermittent shaking. After each incubation period, cells were lysed by adding double-distilled water, and the diluted aliquots were spread on LB agar (*E. coli*) or blood agar (*S. aureus*) plates. Colonies were counted after incubating the plates overnight at 37 °C. Bacterial suspensions without any neutrophils added served as controls for each time point.

***In vivo* bacteria killing assay.** Freshly grown *E. coli* cells were harvested and washed twice with sterile PBS. Eight-twelve week old WT and Selenof KO male mice were challenged by intraperitoneal

injection of *E. coli* with 10^7 cfu in 500 μ l of sterile PBS. Four hours after *E. coli* administration, the animals were euthanized and peritoneal lavage fluid was washed with 10 ml of sterile PBS. The lavage fluid was serially diluted with double-distilled water, then aliquots of serial dilutions were incubated on LB agar plates overnight at 37 °C. The number of colony forming bacteria was counted and the survival rate of *E. coli* determined.

Radioactive pulse and chase assay. Kinetics of IgM biosynthesis and transport were measured with a radioactive pulse-chase assay (Anelli et al., 2002; Cals et al., 1996; Mezghrani et al., 2001).

Intracellular and secreted IgM were measured in primary B cells isolated from WT and Selenof KO mice. At day three of B cell differentiation, cells were incubated for 30 min in DMEM without methionine and cysteine supplemented with 1% dialyzed FCS, pulsed for 15 min with ^{35}S -labeled amino acids (220 $\mu\text{Ci}/10^6$ cells) (Easy Tag, Perkin Elmer), washed and chased in complete medium for the indicated time-points. At time 0, 2, 4 h, the cells were treated with 10 mM NEM to prevent disulfide interchange and lysed in RIPA. Subsequently, lysates were immunoprecipitated with rabbit anti-mouse IgM antibodies (ThermoFisher Scientific #616800), cross-linked to protein G agarose beads. The beads were washed in 0.5 M NaCl, 0.5% SDS, 10 mM Tris-HCl pH 7.5, eluted in Laemmli buffer. Aliquots of the total cell lysates and immunoprecipitates were resolved by SDS-PAGE under non-reducing or reducing conditions and transferred to nitrocellulose. Membranes were then visualized by autoradiography with FLA900 Starion (FujiFilm Life Science, Tokyo, Japan). Densitometric quantification of the signals was performed with ImageJ.

Supplemental References

Anelli, T., Alessio, M., Mezghrani, A., Simmen, T., Talamo, F., Bachi, A., and Sitia, R. (2002). ERp44, a novel endoplasmic reticulum folding assistant of the thioredoxin family. *EMBO J.* 21, 835-844.

Cals, M. M., Guenzi, S., Carelli, S., Simmen, T., Sparvoli, A., and Sitia, R. (1996). IgM polymerization inhibits the Golgi-mediated processing of the mu-chain carboxy-terminal glycans. *Mol. Immunol.* 33, 15-24.

Mezghrani, A., Fassio, A., Benham, A., Simmen, T., Braakman, I., and Sitia, R. (2001). Manipulation of oxidative protein folding and PDI redox state in mammalian cells. *EMBO J.* 20, 6288-6296.